Deutschmann, G., & Ullrich, V. (1979) *Anal. Biochem. 94*, 6–14.
Geraci, G., Parkhurst, L. J., & Gibson, Q. H. (1969) *J. Biol. Chem. 244*, 4664.
Halle, B., Anderson, T., Forsen, S., & Lindman, B. (1981) *J. Am. Chem. Soc. 103*, 500–508.
Kuntz, I. D., Jr., & Kauzman, W. (1974) *Adv. Protein Chem. 28*, 239–345.
Makinen, M. W., Houtchens, R. A., & Caughey, W. S. (1979) *Proc. Natl. Acad. Sci. U.S.A. 76*, 6042–6046.
Maxwell, J. C., Volpe, J. A., Barlow, C. H., & Caughey, W. S. (1974) *Biochem. Biophys. Res. Commun. 58*, 166–171.
Moffat, K., Deatherage, J. F., & Seybert, D. W. (1979) *Science (Washington, D.C.) 206*, 1035–1042.
Rossi Fanelli, A., Antonini, E., & Caputo, A. (1961) *J. Biol. Chem. 236*, 391.
Shimada, H., Iizuka, T., Ueno, R., & Ishimura, Y. (1979) *FEBS Lett. 98*, 290–294.
Squire, P. G., & Himmel, M. E. (1979) *Arch. Biochem. Biophys. 196*, 165–177.
Traylor, T. G., Mitchell, M. J., Tsuchiya, S., Campbell, D. H., Stynes, D. V., & Koga, N. (1981) *J. Am. Chem. Soc. 103*, 5234–5236.
Tsubaki, M., & Yu, N. (1981) *Proc. Natl. Acad. Sci. U.S.A. 78*, 3581.
Tucker, P. W., Phillips, S. E. V., Perutz, M. F., Houtchens, R. A., & Caughey, W. S. (1978) in *Biochemical and Clinical Aspects of Hemoglobin Abnormalities* (Caughey, W. S., Ed.) pp 1–15, Academic Press, New York.
Van Assendelft, O. W. (1970) in *Spectrophotometry of Haemoglobin Derivatives*, Royal Van Gorcum, Ltd., Assen, The Netherlands.
Van Assendelft, O. W., & Zijlstra, W. G. (1975) *Anal. Biochem. 69*, 43–48.
Wang, C. M., & Brinigar, W. S. (1979) *Biochemistry 18*, 4960–4977.
Ward, B., Wang, C. B., & Chang, C. K. (1981) *J. Am. Chem. Soc. 103*, 5236–5238.
Yoshikawa, S., Choc, M. G., O'Toole, M. C., & Caughey, W. S. (1977) *J. Biol. Chem. 252*, 5498–5508.

Chlorophyllide-Substituted Hemoglobin Tetramers and Hybrids: Preparation, Characterization, and Energy Transfer†

Atsuo Kuki and Steven G. Boxer*

ABSTRACT: Three chlorophyllide-substituted human hemoglobin (Hb) complexes have been prepared: the tetrameric complex in which zinc pyrochlorophyllide *a* (ZnPChl*a*) is substituted for all four hemes and the two complementary hybrids in which ZnPChl*a* is substituted for heme in either the α- or β-chains, while heme remains in the other chains. In each of these complexes, intramolecular Chl–Chl singlet energy transfer occurs. A variety of probes demonstrate that ZnPChl*a*–deoxyheme hybrids and the ZnPChl*a*–Hb complexes consistently exhibit properties associated with the well-known T-state tertiary and quaternary structure of deoxyHb itself. Using the known crystal structure of human deoxyHb, we have analyzed the steady-state fluorescence anisotropy of these complexes within the framework of the Förster energy-transfer theory. The result is the determination of the orientation of the Q_y transition dipole moment of ZnPChl*a*. Nuclear magnetic resonance data for the hybrids offer insight into specific tertiary structural changes in the heme pocket surrounding the diamagnetic ZnPChl*a*, which accompany changes in the ligation state of the heme on the opposite chain.

The chlorophyll molecule in nature displays its most important electronic features in structured association with other key components of photosynthetic assemblies. As the intermolecular electronic couplings important in both energy and electron transfer are expected to be highly distance- and orientation-dependent (Förster, 1965; Jortner, 1980), the structure of the molecular assembly undoubtedly exerts control over the fate of the singlet excited state. The existence of a high level of structure has been clearly demonstrated both in bacterial reaction centers [by optical (Rafferty & Clayton, 1979) and magnetic (Boxer & Roelofs, 1979; Thurnauer & Norris, 1976, 1977; Frank et al., 1979) polarization experiments] and in a bacteriochlorophyll-containing light-harvesting antenna complex, whose crystal structure has been determined at high resolution (Matthews & Fenna, 1980). For this reason, it is most appropriate to explore the photophysical and photochemical consequences of specific interchromophore geometries and to test these concepts by the synthesis of model systems.

In response to this challenge, a number of porphyrin and chlorophyll dimers and higher oligomers have been synthesized and characterized in which the structure is defined by specific hydrogen bonding, covalent linkage, and interchromophore π–π association [see Bucks & Boxer (1982) for a review]. In all cases investigated to date, the chlorophylls are in or near to van der Waals contact; consequently, the electron–electron Coulombic repulsion is predicted and observed to produce a strong excitonic interaction (Kasha et al., 1965), and the finite orbital overlap allows the possibility of rapid electron transfer (Netzel et al., 1982).

In this paper we report the synthesis, characterization, and steady-state emission properties of chlorophyll dimers of a completely different sort, possessing interchromophore distances of 25–40 Å. By specific insertion of zinc pyrochlorophyllide *a* (ZnPChl*a*)[1] (Figure 1) into the heme pockets

† From the Department of Chemistry, Stanford University, Stanford, California 94305. *Received December 20, 1982.* This work was supported by grants from the National Science Foundation (PCM-7926677) and the U.S. Department of Energy (DE-FG02-80-CS84006). The 360-MHz NMR spectra were obtained at the Stanford Magnetic Resonance Laboratory, supported by National Science Foundation and National Institutes of Health Grants GR23633 and RR00711, respectively. S.G.B. is an Alfred P. Sloan and Camille and Henry Dreyfus Teacher-Scholar Fellow.

0006-2960/83/0422-2923$01.50/0

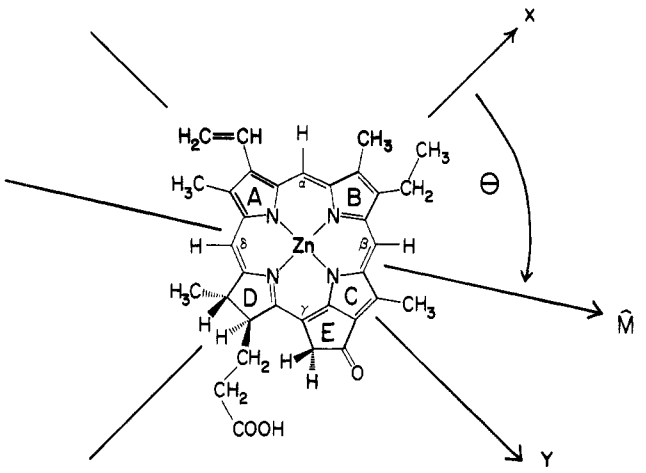

FIGURE 1: Structure of zinc pyrochlorophyllide *a* molecule. By convention, the coordinate system of x and y in-plane axes is as depicted. $\hat{M}$ denotes the unit vector of the transition dipole for the first excited singlet state (often denoted Q_y).

of apohemoglobin (apoHb), we can explore such large interchromophore separations without introducing flexibility or randomness in either the relative distance or orientation. Evidence will be presented to demonstrate that the tertiary and quaternary structures of the ZnPChl*a* complexes are very similar to those of native deoxyHb, whose crystal structure has been determined (Muirhead & Greer, 1970; Bolton & Perutz, 1970). The orbital overlap at these distances is negligible, so energy transfer by an exchange mechanism is expected to be far too slow relative to the singlet lifetime. Indeed, the exchange mechanism does not even appear to participate during the triplet lifetime of the related synthetic protein ZnPPIXHb (Zemel & Hoffman, 1981). The interchromophore distance is also so great that the excitonic interaction is expected to be too weak to maintain coherence. These complexes are in the very weak coupling limit of the interelectronic Coulombic perturbation (Förster, 1965) and are predicted and observed to exhibit Förster resonant energy transfer.

While many ingenious bichromophoric molecules have been studied in which the distance of separation is constrained [e.g., Bücher et al. (1967) and Stryer & Haugland (1967)], only a few systems have also achieved orientational rigidity (Amrein & Shaffner, 1975; Bunting & Filipescu, 1970; Filipescu et al., 1969; Keller, 1968; Lamola, 1969; Tyer & Becker, 1970; Zimmerman et al., 1980). In all these cases, exchange interactions, orientational flexibility, or other complications prevent a quantitative comparison of the theoretical Förster orientational dependence and experiment. In addition, two interesting studies have been reported of energy transfer in ZnPPIX-substituted Hb (Leonard et al., 1974; Zemel & Hoffman, 1981). In these cases, however, a rigorous study of the dipole–dipole orientational dependence of Förster energy transfer is precluded by the intrinsic planar polarization of the porphyrin fluorescent transition (Eaton & Hofrichter, 1981). By contrast, the chlorophyll derivatives have very low symmetry; in combination with the fixed and known interchromophore geometry, the chlorophyll–Hb complexes make an ideal system for quantitative investigations.

The present work is the natural extension of the previously reported detailed studies of 1 to 1 chlorophyllide–apomyoglobin (apoMb) complexes (Boxer & Wright, 1979; Davis & Pearlstein, 1979; Wright & Boxer, 1981). Work from our laboratory showed that various chlorophyllides and zinc bacteriochlorophyllide could be reconstituted into the heme pocket of apoMb and that the binding was specific. Crystallization of the complex leads to a system with many chromophores in an ordered array (Boxer et al., 1982). The apoHb molecule, when fully reconstituted with ZnPChl*a*, offers a system for the study of four chlorophyllides of fixed mutual orientation, $\alpha_2^{Chl}\beta_2^{Chl}$.[2] Molecular systems containing two chlorophyllides can be obtained by the synthesis of Hb hybrids. Tetrameric hybrids have been prepared which contain deoxyhemes in the α-chains and ZnPChl*a* in the β-chains, α_2^{h}(deoxy)β_2^{Chl}, as well as the complementary combination, $\alpha_2^{Chl}\beta_2^{h}$(deoxy).[2] As energy transport can be studied most unambiguously in the case of only two chlorophylls, where there is only one transfer rate constant, these hybrids will be the subject of the most detailed analysis.

Energy transfer occurs between identical monomers in these systems; consequently, the widely used technique of fluorescence depolarization is the appropriate methodology (Albrecht, 1961). The excitation must be tuned into the same electronic state that fluoresces in order to avoid the phenomenon that interested Albrecht, namely, the differing polarizations of different electronic states. We report here the steady-state fluorescence depolarization results and will present time-resolved polarization measurements in a subsequent paper. From an analysis of the steady-state results, we can predict the orientation of the Chl Q_y transition dipole moment within the molecular frame (the angle θ in Figure 1). This will be compared with results obtained theoretically (Chang, 1977; Petke et al., 1979; Weiss, 1972), which have never been directly verified by experiment [see Boxer et al. (1982) for one attempt]. This orientation is the cornerstone of all interpretations of polarized light spectroscopy or excitonic interactions in natural chlorophyll-containing systems in terms of their molecular architecture.

Finally, we note that the X-ray structure is known for only one photosynthetic protein at this time, the bacteriochlorophyll protein from *Prosthecochloris aestuarii* (Matthews & Fenna, 1979). Fenna and Matthews emphasize that the organization of bacteriochlorophyll in the complex is determined by chlorophyll–protein interactions, including ligation to the metal atom, hydrogen bonding, and hydrophobic interactions, and *not* by direct chlorophyll–chlorophyll self-association. The work presented in this paper is a first step in the direction of designing well-defined, multichlorophyll, macromolecular complexes.

Experimental Procedures

Preparation of Chromophore. Pyropheophorbide *a* was prepared from spinach by standard methods (Strain & Svec, 1966). Zn was inserted (Furhop & Smith, 1975), and the purity of ZnPChl*a* was verified by TLC (9/1 CH_2Cl_2/CH_3OH, $R_f \sim 0.3$). Zn was used due to its ease of insertion, the stability of ZnPChl*a*, and the well-established similarity between zinc and magnesium chlorophyllides.

Purification of Hb. OxyHb was obtained from human blood by the standard procedure (Antonini & Brunori, 1971), fol-

[1] Abbreviations: DEAE, diethylaminoethyl; Me_2SO, dimethyl sulfoxide; Hb, human hemoglobin; ICP, inductively coupled plasma; Mb, sperm whale myoglobin; PMB, *p*-mercuribenzoate; ZnPPIX, zinc protoporphyrin IX; ZnPChl*a*, zinc pyrochlorophyllide *a*; Tris, tris(hydroxymethyl)aminomethane; EDTA, ethylenediaminetetraacetic acid; Bis-Tris, [bis(2-hydroxyethyl)amino]tris(hydroxymethyl)methane.

[2] For compactness, we adopt the following standard shorthand notation for reconstituted Hb's: $\alpha_2^{Chl}\beta_2^{h}$(deoxy) has ZnPChl*a* in both α-chains and heme, in the deoxy form, in both β-chains. Superscript 0 indicates apochains.

lowed by batch purification with ion-exchange DEAE-cellulose (Whatman DE-52) (Hinson & McMeekin, 1969). The absence of trace amounts of HbA_2 was verified by electrophoresis on cellulosic mylar strips (Gelman Super Sepraphore) in 0.18 M Tris–borate buffer (pH 8.6) containing 3 mM EDTA. The purified oxyHb was stored at 4 °C. ApoHb was prepared at 0 °C from cyanometHb by Teale's acid–butanone method (Teale, 1959). The globin solutions were always taken directly to the next step.

Preparation of ZnPChla–Cyanomet-heme Hybrids. Two successful routes to the hybrids were found. One was used for the preparation of $\alpha_2^{Chl}\beta_2^{h}$(CN·met) and the other for the preparation of α_2^{h}(CN·met)β_2^{Chl}.

$\alpha_2^{h}(CN{\cdot}met)\beta_2^{Chl}$. Semihemoglobin, containg heme in only the α-chains, α^{h}(CN·met)β^{0}, was prepared according to the method of Winterhalter (1966). This protein is known as ICII and, if kept in cyanomet form with 100 mg of KCN/L in all buffers, suffers no heme exchange into the unoccupied pockets of the β-chains (Winterhalter & Deranleau, 1967). Purification of ICII was achieved as described by Winterhalter [a 1 × 15 cm CM-52 (Whatman) ion-exchange cellulose column sufficed to give excellent resolution]. The ICII is electrophoretically indistinguishable from the direct alloplex recombination product of the α-cyanomet chain and β-globin chains (Waks et al., 1973), reproducibly exhibiting an anodic mobility 78 ± 1% of that of cyanometHb.

Insertion of ZnPChl*a* into ICII was accomplished as follows (buffer was 20 mM phosphate, pH 7.4–100 mg of KCN/L, 20 °C, throughout). Two 2.5 × 8 cm S-200 (Pharmacia) columns were equilibrated with buffer. A 3–4-fold excess of ZnPChl*a* was dissolved in 0.5 mL of Me_2SO and then diluted with 0.5 mL of buffer and immediately loaded onto one of the S-200 columns. The green band spread down and then stopped as the Me_2SO was diluted, coloring the top 1.5 cm of the column dark green. The column was then washed with 2 column volumes of buffer to eliminate the Me_2SO. A 0.5–1% solution of ICII was then loaded onto the top of the column and allowed to enter at 0.2 mL/min until all of the red solution had entered the column. Elution was continued at this rate for 30 min; then, the dark green protein was eluted from the column. Typically, the visible spectrum of the protein at this stage revealed a red tail on the Q_y chlorophyll band and a ratio of OD at 700 to 661 nm (peak) of ~0.02. This red tail was eliminated by passing the protein through the clean S-200 column. This removed all nonspecifically bound chromophores, giving a ratio $OD_{700}/OD_{661} < 0.005$, and the Q_y band displayed a full width at half-maximum of 19 nm. Gelman cellulose electrophoresis confirmed that there was no starting ICII remaining.

$\alpha_2^{Chl}\beta_2^{h}(CN{\cdot}met)$. The α- and β-chains of purified oxyHb were cleaved with *p*-mercuribenzoate (PMB), separated, and regenerated to the free sulfhydryl form by literature procedures at 4 °C (Yip et al., 1977; Geraci et al., 1969). Purity of the free sulfhydryl chains was ascertained by cellulosic electrophoresis.

We report a new variation of the technique for preparing α- and β-globin chains in higher yield than reported before (Waterman & Yonetani, 1970; Alpert, 1972; Friedman et al., 1981). Concentrated stock solutions of KCN and $K_3Fe(CN)_6$ and a desalting column (Bio-Gel P6DG) were prepared, all in 20 mM phosphate, pH 7.4. Five equivalents of KCN were added to a 1% solution of oxy α- or β-chains at 4 °C followed by 3 equiv of the ferricyanide. The mixture was left for 1.5 h in the cold. Due to the presence of cyanide, no precipitation was observed. The ferro- and excess ferricyanide were removed by passing the protein through the P6DG column. The hemin was then extracted with the standard acid–butanone technique (Yonetani, 1967; Teale, 1959) at pH 2.2. The clear aqueous layer was then passed through a P6DG column equilibrated in 20 mM phosphate, pH 5.7, with 1 mM EDTA and 1 mM dithioerythritol at 4 °C to eliminate the residual butanone; yield 97+%.

The α^0 solution thus obtained was mixed in 1:1 mole ratio with cyanomet β-chain in 20 mM phosphate, pH 5.7, containing 100 mg/L KCN. This standard alloplex recombination (Yip et al., 1977) produces appreciable amounts of the semihemoglobin $\alpha^0\beta^h$(CN·met) in 3 h. Purification was accomplished with a 1 × 5 cm CM-52 column, as described above for ICII, except that the nonlinear gradient used contained 50% higher buffer concentrations throughout. The electrophoretic purity of the $\alpha^0\beta^h$(CN·met) was checked; its anodic mobility was consistently 71 ± 2% of that of cyanometHb, making it readily distinguishable from ICII.

Reconstitution of ZnPChl*a* into the empty α-chain pockets to produce $\alpha_2^{Chl}\beta_2^{h}$(CN·met) was accomplished exactly as with α_2^{h}(CN·met)β_2^{Chl}.

$\alpha_2^{Chl}\beta_2^{Chl}$. The two-column S-200 method as described above was used at pH 5.7. It is interesting that the $\alpha_2^{Chl}\beta_2^{Chl}$ produced by this method is found to contain the full complement of four ZnPChl*a* molecules per protein tetramer. Furthermore, the PMB reaction does not work on $\alpha_2^{Chl}\beta_2^{Chl}$.

Conversion to Deoxy Hybrids. The reduction of Fe(III) by dithionite was always accomplished just before the ferrous form was required for an experiment. Optical and gel-filtration samples were reduced by the addition of freshly prepared 1% sodium dithionite stock solution to a degassed solution of ~0.1% hybrid. The color changed immediately from an olive-green to a blue-green. NMR samples were prepared free of dithionite so that they could be successively oxygenated, deoxygenated, and reoxygenated in the tube by equilibration with O_2 or Ar. The cyanomet hybrids were first concentrated by ultrafiltration (Amicon PM-10) to ~1% under Ar. The dithionite was added and the mixture stirred for 15 min in the Amicon cell. This was then further concentrated to the minimum volume possible and passed through three cycles of dilution with D_2O and concentration to the minimum volume. Samples for NMR were 1% in 10 mM deuterated phosphate buffer, pH 7.0.

Small-zone gel-filtration experiments were performed on the deoxy hybrids with a 1.5 × 20 cm column of Sephadex G-75 (Pharmacia) in 20 mM Bis-Tris-HCl, pH 7.0 at 4 °C. On this column, a sample of carbon monoxide Hb, which is 100 μM (per chain) when loaded, exhibits a 23% broader elution band than a sample of deoxyHb at 50 μM concentration. The deoxyHb at this concentration is completely tetrameric (Chu & Ackers, 1981). Thus, the column is capable of detecting the partial equilibrium dissociation of the carbon monoxide Hb sample, though the initial-chain concentration is 40 times the dissociation constant (Kirshner & Tanford, 1964). This is used as a guide in the estimation of the upper bound for the dissociation constant of our deoxy hybrids. Large-zone gel-filtration experiments were performed on $\alpha_2^{Chl}\beta_2^{Chl}$ after the method of Ackers (1967). A Sephadex G-100 column equilibrated with 50 mM Bis-Tris-HCl, pH 7.0, was used, both with and without an additional 400 mM $MgCl_2$ as a promoter of dissociation (Guidotti, 1967).

Chemical Analyses. The reactive sulfhydryls of the hybrids in their aquomet forms were titrated with PMB according to the method of Boyer (1954). The PMB was added both to the sample cuvette and to a reference cuvette containing a

solution of horse heart myoglobin of identical volume and absorption at 250 nm. PMB concentrations were determined by the absorbance at 233 nm [ϵ_{233} = 17400 M^{-1} cm^{-1} (Hwang & Greer, 1980)].

Stopped-flow measurements of the PMB reaction were performed with a PMB concentration of 1.16×10^{-4} M and a β93-SH concentration of 1.2×10^{-5} M or less. The proteins were in 20 mM phosphate, pH 7.0 at 22 °C, and the hybrids were measured in their deoxy states. The reduction of the cyanomet hybrids to their deoxy ferrous forms was accomplished with a 10-fold excess of $Ru^{II}(NH_3)_6Cl_2$. This reagent does not absorb significantly at the observation wavelength (250 nm). Elemental analyses for iron and zinc in the hybrids were performed by the standard ICP technique.

Steady-State Fluorescence. A 90° fluorescence spectropolarimeter was built from an RCA C31034 PM tube, a 600-W quartz–halogen lamp, two Spex Doublemate double monochromators with 750-nm blaze gratings on the emission side, and a Spex DPC-2 photon-counting apparatus. These gratings exhibit very little polarization bias in the spectral region of chlorophyll fluorescence. Particular attention was paid to restricting the angle of convergence of the excitation beam and the collection angle of the emission lens, both of which can lead to erroneously low polarization values. Glan-Thompson prism polarizers were used with an extinction of $>10^{-6}$.

Measurements of fluorescence polarized parallel or perpendicular to the excitation polarization were interleaved to cancel the effects of minor sample degradation, though this generally proved unnecessary. The residual polarization bias of the emission-detection system was measured by using methanolic solutions of oxazine 725 or ZnPChl*a* and horizontally polarized excitation light at a variety of wavelengths. The absolute accuracy of the anisotropies measured by the instrument was determined with a glycogen suspension (Eastman Kodak), which is ideally a completely polarized scatterer. Any perpendicularly polarized light detected (above that of the H_2O blank) was assigned to instrumental imperfection and is reported in the results.

Rigorously anaerobic samples were prepared by Schlenk-line and cannula and septa techniques. Protein solutions were prepared in 50 mM Bis-Tris-HCl, pH 7.0, and 50% sucrose and contained 0.05% dithionite from the prior reduction step in the case of the deoxyheme hybrids. The fluorometry cell was a 10 × 4 mm septum-capped jacketed quartz flow cell; coolant circulated through the jacket. Macromolecular rotation in this buffer was minimal at room temperature and was eliminated completely by cooling to 10 °C, where the fluorescence anisotropy of ZnPChl*a*–Mb reached a constant maximum value. All final measurements were made at 0–5 °C, at which temperature the viscosity of the solution is >30 cP. The possibility of intermolecular energy transfer and of secondary reabsorption and emission was eliminated by working at low concentration (≤2 μM, OD_{661}^{4mm} <0.04).

Results

Characteristics of Hybrid Proteins. The visible absorption spectra of $\alpha_2^{Chl}\beta_2^{Chl}$ and $\alpha_2^{h}(deoxy)\beta_2^{Chl}$ are shown in Figure 2. The absorption spectrum of the latter is almost indistinguishable from that of the complementary hybrid. A small difference is observed between the ratios of the peak height of the combined heme–ZnPChl*a* Soret band and the peak height of the ZnPChl*a* Q_y band; this ratio is 3.21 for $\alpha_2^{Chl}\beta_2^{h}(deoxy)$ and 3.59 for $\alpha_2^{h}(deoxy)\beta_2^{Chl}$. The extinction coefficients determined by ICP Zn analysis of samples of known absorbance agree very well with the result from PMB

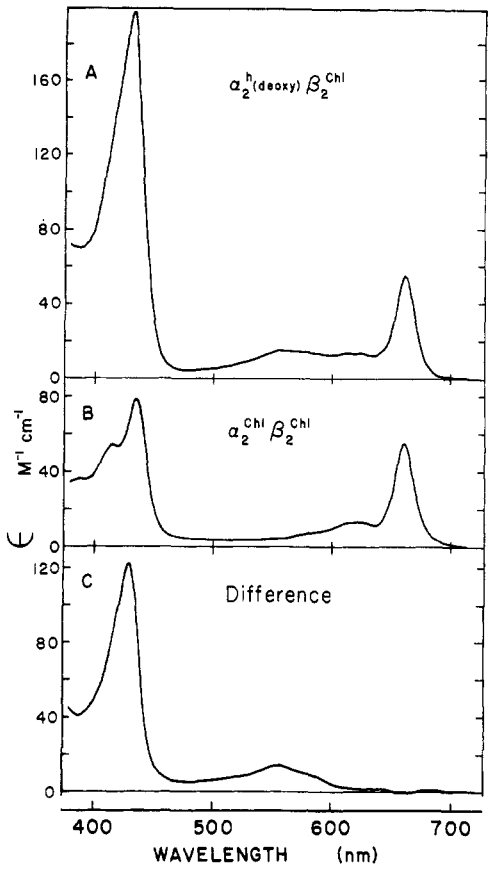

FIGURE 2: Electronic absorption spectra of (A) $\alpha_2^{Chl}\beta_2^{Chl}$ and (B) $\alpha_2^{h}(deoxy)\beta_2^{Chl}$. The difference spectrum (B − A), where the absorbance at the peak of the Q_y bands has been matched, is presented in (C).

titration of the reactive β93-sulfhydryls: ϵ_{661} = 58000 ± 3000 M^{-1} cm^{-1} for $\alpha_2^{Chl}\beta_2^{h}(deoxy)$ and ϵ_{661} = 55000 ± 3000 M^{-1} cm^{-1} for $\alpha_2^{h}(deoxy)\beta_2^{Chl}$.

The spectra of the hybrids are the sum of the spectra of $\alpha_2^{Chl}\beta_2^{Chl}$ and native Hb in all forms of hybrid measured: deoxy, oxy, and cyanomet. The difference spectrum [$\alpha_2^{h}(deoxy)\beta_2^{Chl} - \alpha_2^{Chl}\beta_2^{Chl}$] is shown in Figure 2C. The peak of the Soret band in the difference spectrum of both hybrids is at 430 nm with a full width at 90% of maximum of 9 nm. This is exactly the same as T-state deoxyHb and is more intense, sharper, and slightly red shifted with respect to isolated α- or β-chains in the deoxy state (Soret-band maximum at 429 nm, full width at 90% of maximum of 12 nm). Using ϵ_{430} = 133000 M^{-1} cm^{-1} for deoxyHb (Antonini & Brunori, 1971) and the difference spectrum, we can estimate the ratio of heme to ZnPChl*a* chromophore as 0.91 ± 0.1 for $\alpha_2^{Chl}\beta_2^{h}(deoxy)$ and 0.98 ± 0.1 for $\alpha_2^{h}(deoxy)\beta_2^{Chl}$, which supports the expected 1:1 stoichiometry.

The Fe to Zn stoichiometry, as determined by elemental analysis on 1 mg of protein, was 0.9 ± 0.1 to 1 for both $\alpha_2^{h}(deoxy)\beta_2^{Chl}$ and $\alpha_2^{Chl}\beta_2^{h}(deoxy)$. Both hybrids in the deoxy state and $\alpha_2^{Chl}\beta_2^{Chl}$ elute as tetramers in the gel-filtration experiments and remain tetrameric with no evidence of dissociation to below 2 μM concentration (per chain). We conservatively estimate that an upper limit for the dissociation constant, K_D, is 5×10^{-8} M. The elution profile of $\alpha_2^{Chl}\beta_2^{Chl}$ in the large-zone gel-filtration experiments is indistinguishable from that of a tetramer, even at 0.8 μM concentration (per chain) and whether or not 400 mM $MgCl_2$ is present. Since a 10% equilibrium population of dimers would be readily detectable, we conclude that the dissociation constant must be less than 1×10^{-8} M. This upper limit is 60000 times less

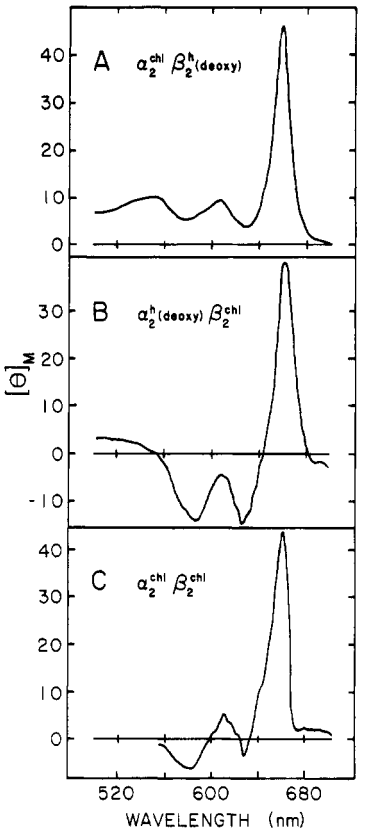

FIGURE 3: Comparison of circular dichroism spectra of (A) $\alpha_2^{Chl}\beta_2^{h}$(deoxy), (B) α_2^{h}(deoxy)β_2^{Chl}, and (C) $\alpha_2^{Chl}\beta_2^{Chl}$ at 20 °C.

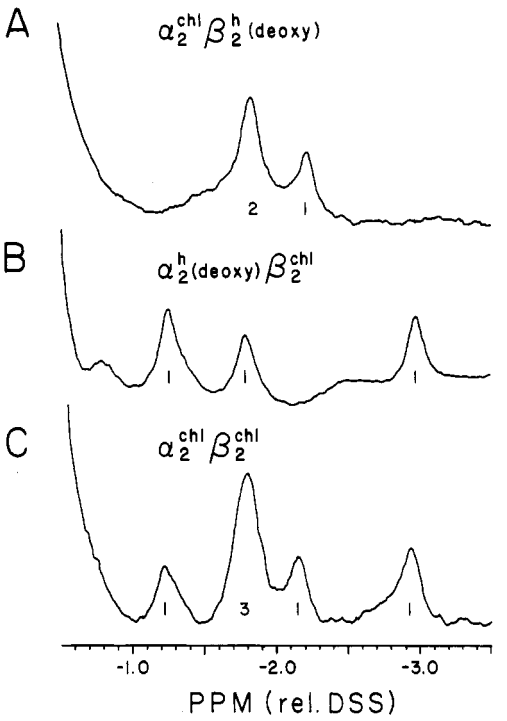

FIGURE 4: ^{1}H NMR spectra (360 MHz) in upfield region of (A) $\alpha_2^{Chl}\beta_2^{h}$(deoxy), (B) α_2^{h}(deoxy)β_2^{Chl}, and (C) $\alpha_2^{Chl}\beta_2^{Chl}$. All samples are ca. 10^{-3} M in 10 mM deuterated phosphate, pH 7, at 31 °C. The ratios of the integrals are denoted under the peaks and are ±15%.

than the dissociation constant observed for oxyHb in 400 mM $MgCl_2$ (Guidotti, 1967).

The measured pseudo-first-order rate constant for the PMB reaction of oxyHb was 60 times faster than that for deoxyHb under the same conditions. This is in agreement with the original result (Antonini & Brunori, 1969). Under these conditions, α_2^{h}(deoxy)β_2^{Chl} exhibits a reaction rate 10% slower than that of deoxyHb, and $\alpha_2^{Chl}\beta_2^{h}$(deoxy) exhibits a rate 50% faster than that of deoxyHb. These are small differences relative to the very large difference in reactivity between oxy- and deoxyHb.

Heme to ZnPChl*a* energy transfer within the hybrid does not occur, as demonstrated by the fluorescence excitation spectra for $\alpha_2^{Chl}\beta_2^{Chl}$, α_2^{h}(deoxy)β_2^{Chl}, and $\alpha_2^{Chl}\beta_2^{h}$(deoxy), which are nearly superimposable. This is not surprising, as the excited states of heme possess subpicosecond lifetimes (Adar et al., 1976) that are far too short for Förster energy transfer to occur.

The circular dichroism spectra of the proteins are presented in Figure 3 for the Q-band region. The main positive feature at 660 nm is essentially the same in α_2^{h}(deoxy)β_2^{Chl}, $\alpha_2^{Chl}\beta_2^{h}$(deoxy), $\alpha_2^{Chl}\beta_2^{Chl}$, and ZnPChl*a*–Mb (Wright & Boxer, 1981) and is in all cases opposite in sign from monomeric ZnPChl*a* in an organic solvent (Wright & Boxer, 1981). From 640 to 560 nm, the CD of $\alpha_2^{Chl}\beta_2^{h}$(deoxy) and α_2^{h}(deoxy)β_2^{Chl} differ in sign, though the peaks and troughs occur at roughly the same wavelength. It is noteworthy that the CD pattern of $\alpha_2^{Chl}\beta_2^{Chl}$, containing four ZnPChl*a*'s, is essentially the same as the sum of the CD spectra of α_2^{h}(deoxy)β_2^{Chl} and $\alpha_2^{Chl}\beta_2^{h}$(deoxy) in this region.

NMR. Aside from the CD spectrum, the most dramatic difference between the two hybrids appears in the upfield region of their NMR spectra. This upfield region is shown in Figure 4, and consists of diamagnetic ring current shifted protein methyl groups, by analogy with extensive previous work (Lindstrom et al., 1972; Shulman et al., 1970). Methyl protons close to the paramagnetic Fe(II) of the deoxyheme are expected to be very broad at 360 MHz (Guéron, 1975; Johnson et al., 1977) and do not occur in the 0 to −8 ppm region. Thus, in the deoxy hybrids, we only expect to see protein methyl resonances from the heme pocket of the chain containing the diamagnetic ZnPChl*a*. In the diamagnetic oxyheme form, we also expect to see an upfield-shifted Val-E11 methyl from the heme-containing pocket. The upfield-shifted peaks of the NMR spectrum of $\alpha_2^{Chl}\beta_2^{Chl}$ are spread out over a 3 ppm range, and the integrals indicate that six methyl groups per $\alpha\beta$ half of the tetramer must be accounted for; the other half is related by C_2 symmetry. This is in sharp contrast to the case of oxyHb, which displays one peak in this region, due to overlapping E11-valine methyl resonances from the α- and β-chains (Ho, 1981).

Comparing the spectra, one sees immediately that the four-peak pattern of $\alpha_2^{Chl}\beta_2^{Chl}$ is given exactly by the sum of the two-peak (three methyl) $\alpha_2^{Chl}\beta_2^{h}$(deoxy) spectrum and the three-peak (three methyl) α_2^{h}(deoxy)β_2^{Chl} spectrum. The following assignment of the $\alpha_2^{Chl}\beta_2^{Chl}$ peaks is logically irresistible: −1.29 ppm (one β-chain methyl), −1.86 ppm (one β-chain methyl, two α-chain methyls), −2.21 ppm (one α-chain methyl), −3.03 ppm (one β-chain methyl).

Fluorescence Anisotropy. Fluorescence anisotropy is defined as $r = (I_\parallel - I_\perp)/(I_\parallel + 2I_\perp)$ where $I_\parallel$ and $I_\perp$ are the emission intensities (corrected for the emission polarization bias of the instrument) polarized parallel and perpendicular, respectively, to the polarization of the excitation beam. The emission polarization bias ($\parallel/\perp$) of the fluorometer at 670 nm was determined to be 0.955 ± 0.002 and is near unity. The absolute accuracy of the measured anisotropies is reflected in the high anisotropies observed for the glycogen scatterer: r = 0.983 ± 0.003 (r = 1 for an ideally isotropic scatterer) and r = 0.385 ± 0.003 for oxazine 725 in glycerol (the theoretical maximum for a fluorophore is r = 0.4). The fluorescence anisotropies observed for α_2^{h}(deoxy)β_2^{Chl}, $\alpha_2^{Chl}\beta_2^{h}$(deoxy),

Table I: Experimentally Determined Polarization Anisotropies for ZnPChl*a* Fluorescence in Several Protein Complexes

protein	anisotropy[a]
$\alpha_2^{Chl}\beta_2^{h}$(deoxy)	0.289 ± 0.005
α_2^{h}(deoxy)β_2^{Chl}	0.287 ± 0.003
$\alpha_2^{Chl}\beta_2^{Chl}$	0.178 ± 0.004
ZnPChl*a*-Mb	0.366 ± 0.002
ZnPChl*a*-Mb[b]	0.348 ± 0.004
ZnPChl*a*-Mb[c]	0.352 ± 0.005

[a] λ_{ex} = 662 nm, λ_{em} = 670 nm, and slit width = 3 nm, unless otherwise noted. [b] λ_{ex} = 653 nm; λ_{em} = 670 nm. [c] λ_{ex} = 662 nm; λ_{em} = 680 nm.

$\alpha_2^{Chl}\beta_2^{Chl}$, and ZnPChl*a*–Mb are presented in Table I. ZnPChl*a*–Mb has the highest anisotropy, $\alpha_2^{Chl}\beta_2^{Chl}$ has the lowest, and the deoxy hybrids are intermediary. The anisotropy of ZnChl*a*–Mb is defined as the monomer anisotropy r_0: $r_0 = 0.366 \pm 0.002$.

In order to measure depolarization due to energy transfer, it is imperative that any instrumental depolarization be negligible, and this is demonstrated by the result for glycogen. The anisotropy observed for the monomeric ZnPChl*a*–Mb (Table I) is somewhat higher than other values reported in the literature for chlorophyll (Bär et al., 1961; Gouterman & Stryer, 1962; Sevchenko et al., 1968; Koka & Song, 1977), though measurably less than that for oxazine 725. Narrowing the monochromator slits and exciting at 664 nm and observing at 670 nm does not alter the observed anisotropy within the experimental uncertainty; however, the anisotropy does fall from this maximum value by a small, but significant, amount when exciting at 653 nm or observing at 680 nm (Table I). Note that these effects occur while staying well within the strong 0–0 vibronic band of the Q_y transition; the implication of this is discussed under Appendix.

Discussion

Chlorophyllide–heme hybrids of hemoglobin have been prepared in which intramolecular chlorophyll–chlorophyll singlet energy transfer occurs. The advantage of this approach over others (Knox, 1975; Seely, 1970) is that the relative geometry of each interacting pair of chlorophyllides is constant. However, the successful analysis of the fluorescence anisotropy data places stringent requirements on the prior characterization of the proteins, beyond the simple determinations of stoichiometry and purity. Through a variety of probes of solution conformation, we will show that the ZnPChl*a*–deoxyheme hybrids exhibit the well-known T-state tertiary and quaternary structure of deoxyhemoglobin [comparable conformational probes have been used in Mn, Co, and ZnPPIX Hb (Hoffman, 1979)]. We will then proceed to use the crystal-structure coordinates for human deoxyhemoglobin (Perutz, 1970),[3] assuming complete structural homology with the ZnPChl*a*–deoxyheme hybrid. The result is the determination of the orientation(s) of the Q_y transition dipole moment of chlorophyll, which, in part, controls the orientational dependence of any electronic interaction with the lowest singlet excited state of chlorophyll.

As the hemoglobin frame is used to elucidate energy transfer among chlorophylls, so the ZnPChl*a* molecule also serves as a probe of hemoglobin conformation, particularly in the NMR spectra of the hybrids. We will briefly note below, as a small contribution to a vast literature (Antonini & Brunori, 1971; Ho & Russu, 1981), the observed correlation of specific tertiary structural changes with the state of oxygenation of the two ferrous hemes in the hybrids, though the bulk of this discussion is postponed to a future paper.

Stoichiometry and Purity. The Fe to Zn stoichiometry and the analysis of the hybrid optical absorption spectra in terms of heme to ZnPChl*a* chromophore ratio confirm a one-to-one stoichiometry for both $\alpha_2^{h}\beta_2^{Chl}$ and $\alpha_2^{Chl}\beta_2^{h}$ hybrids. The very good agreement between the extinction coefficient of the ZnPChl*a* Q_y band as determined by Zn analysis and by titrating the β-chains with PMB indicates that both hybrids are fully reconstituted with ZnPChl*a*. The electrophoretic purity of the hybrids and their precursor semihemoglobins and comparison of the deoxy NMR spectra (Figure 4A,B) show that neither sample is contaminated by hybrids of the opposite type.

Tertiary and Quaternary Structure. Zinc porphyrins and chlorins bind a fifth ligand to form pentacoordinate complexes but will not bind a sixth ligand under ordinary conditions (Buchler, 1975). Thus, as in the case of ZnPPIX Hb (Hoffman, 1979), the replacement of two or four pentacoordinate deoxyhemes in hemoglobin by ZnPChl*a* might be expected to leave the proteins in the T-state conformation.

The optical difference spectra (e.g., Figure 2C) reveal that the deoxyheme Soret bands of both hybrids exhibit the characteristic shape of the T-state tetrameric deoxyHb Soret. This is distinct from the other type of Soret band observed in the spectra of isolated, deoxygenated α- and β-chains, as well as in the quickly reacting, high ligand affinity R-state forms of modified deoxyhemoglobins (Antonini & Brunori, 1971). Thus, using the electronic structure of the deoxyhemes as a probe, we conclude that the hybrids appear to be in the tetrameric T state.

In addition, the gel-filtration results demonstrate that the deoxy hybrids possess an extremely low dimer–tetramer dissociation constant, which is at least 50 times smaller than the value for R-state oxyhemoglobin [$K_D = 2.5 \times 10^{-6}$ mol L^{-1} under similar conditions (Antonini & Brunori, 1971)]. The dissociation constant of deoxyhemoglobin is estimated at 10^{-10} M (Chu & Ackers, 1981); this tighter association is most likely the consequence of six new interchain salt bridges that must be broken to allow the protein to adopt the R conformation (Perutz, 1970). The very tight association of the deoxy hybrid tetramers is direct evidence that the *quaternary* structure of the hybrids is like that of T-state Hb and distinctly different from that of R-state Hb.

The reactivity of the β93-cysteine sulfhydryls to the PMB reagent is a probe of the structure of the $\alpha_1\beta_2$ interface of Hb that distinguishes oxy- from deoxyhemoglobin. Again, the deoxy hybrids show deoxy- rather than oxyhemoglobin behavior.

Finally, the ultimate test of the hypothesis that our compounds possess the T-state geometry is the self-consistency among the independent results for the calculation of the ZnPChl*a* transition dipole orientation, θ (Figure 1), from three different fluorescent proteins, α_2^{h}(deoxy)β_2^{Chl}, $\alpha_2^{Chl}\beta_2^{h}$(deoxy), and $\alpha_2^{Chl}\beta_2^{Chl}$, discussed below.

Circular Dichroism. The circular dichroism data for the tetramer containing four ZnPChl*a*'s are essentially the sum of the two deoxy hybrids' CD spectra for the red-most bands. ZnPChl*a* is an asymmetric chromophore, and the CD for the monomer Q_y transition is negative. This intrinsic CD is more than equaled by positive CD due to coupled oscillator interactions with nearby amino acids when the chromophore is

[3] Deoxyhemoglobin coordinates were obtained at the Computer Graphics Laboratory (University of California at San Francisco) with data from the Brookhaven Protein Data Bank (Bolton & Perutz, 1970).

We thank Professors Langridge and M. F. Perutz for their generous assistance.

embedded in the protein. We have observed exactly the same effect in ZnPChl*a*–Mb, with a comparable magnitude (Boxer & Wright, 1979; Wright & Boxer, 1981). Apparently, those aromatic amino acids that make the largest contribution are comparably positioned in α- and β-chains of human globin and in sperm whale apoMb. The region to the blue of the Q_y transition contains both the deoxyheme visible bands and the ZnPChl*a* Q_x transitions. These features are of opposite sign in the CD of the two hybrids and the peak maxima are offset. We have similarly observed much larger variations in the sign and intensity of CD in this region for apoMb substituted with a number of different chlorophyll derivatives (Wright & Boxer, 1981). This weak CD is the sum of many large offsetting components, so this is a sensitive and diagnostic region, but further analysis is not warranted.

We would not expect any exciton coupling between these ZnPChl*a* chromophores, and indeed, there is no evidence of a conservative, split component in the CD spectra (Figure 3). Thus, there is no exciton interaction within the α–α or β–β pairs of ZnPChl*a* chromophores in the hybrids, and the fact that the tetramer is the sum of the hybrids shows that there is no α–β chain interchromophore excitonic interaction.

^1H NMR. The application of proton NMR to the study of the structure of partially ligated Hbs has led to a great expansion in the understanding of the cooperative mechanism of oxygen binding (Ho & Russu, 1981; Ogawa & Shulman, 1972). In particular, hybrids offer a selective approach to monitoring allosteric interactions among the chains. The hybrid is designed to have an NMR probe in one kind of chain, which will not change its state of ligation while the state of ligation in the opposite chains is switched. Principal examples of this approach include Fe(III)CN–Fe(II) hybrids of many kinds (Ogawa & Shulman, 1972) and Co(II)–Fe(II) hemoglobins (Ikeda-Saito et al., 1978).

The NMR spectra of ZnPChl*a* hybrids offer new information. Unlike cyanomet-, oxy-, or carbon monoxide heme, the zinc chlorin is five-coordinate; thus these hybrids can be used to study the transition from a fully unligated to a doubly ligated Hb (Hoffman, 1979). Unlike deoxy ferrous (Ho & Russu, 1981), cobaltous (Ikeda-Saito et al., 1978), or manganous (Hoffman, 1979) hemes, ZnPChl*a* is always diamagnetic, and upfield ring current shifts of nearby protein methyl protons can be observed. This is significant because it provides direct information on the motion of protein residues in the unligated heme pocket, where components of the allosteric mechanism may be detectable. ZnPPIX–heme hybrids have been prepared (Leonard et al., 1974) that are also diamagnetic and five-coordinate in the probe sites, but NMR studies of these proteins have not appeared in the literature. The NMR spectrum of ZnPPIXHb shows a rich upfield region with peaks from −1.8 to −4.1 ppm (A. Kuki and S. G. Boxer, unpublished results), which indicates that the pursuit of ZnPPIX hybrid NMR may be promising. This also suggests that the profusion of upfield peaks in our ZnPChl*a* hybrids is due to the T-state conformation of the protein rather than to the differences between chlorin and porphyrin ring currents.

The upfield region in the NMR of the oxygenated hybrids, $\alpha_2^{h}(\text{oxy})\beta_2^{Chl}$ and $\alpha_2^{Chl}\beta_2^{h}(\text{oxy})$, is indeed distinctly different from the spectra presented in Figure 4 for the same proteins in the deoxygenated state. Briefly, there are more dramatic changes in the tertiary structure of the heme crevice around the ZnPChl*a* probe, as judged by NMR, in the case of $\alpha_2^{Chl}\beta_2^{h}(\text{oxy})$ than in $\alpha_2^{h}(\text{oxy})\beta_2^{Chl}$. This data will be presented, along with tentative peak assignments, in a separate paper.

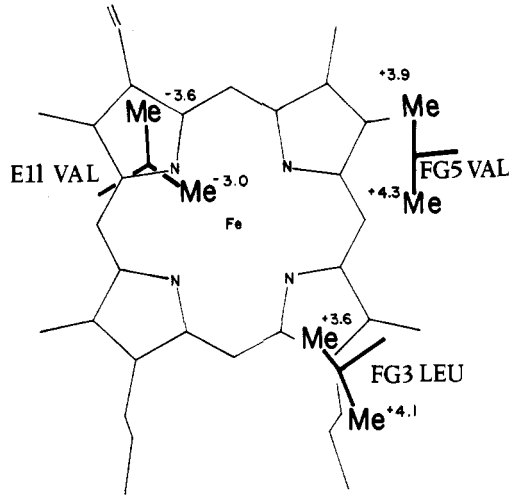

FIGURE 5: Illustration of nearby protein methyl groups in the heme pocket in the β-chain of deoxyhemoglobin. The amino acids are shown in projection on the heme plane, and the vertical distances from the heme plane are shown in angstroms. A positive value indicates that the residue is on the proximal side. These positions are calculated from the crystal structure data of Perutz.[3]

As mentioned previously, the upfield spectrum of $\alpha_2^{Chl}\beta_2^{Chl}$ is the exact superposition of the spectra of $\alpha_2^{Chl}\beta_2^{h}(\text{deoxy})$ and $\alpha_2^{h}(\text{deoxy})\beta_2^{Chl}$. This means that there is no NMR evidence for a structural change when the deoxyheme in the *opposite* chain is replaced by a ZnPChl*a* chromophore. This is a necessary condition for the assertion that there is homology in the manner in which the protein folds around ZnPChl*a* and heme.

To proceed with the analysis, we must propose a tentative assignment of the α- and β-chain methyl proton peaks in the upfield region of the ZnChl*a*–heme (deoxy) hybrids to specific amino acids, using the T-state deoxyhemoglobin crystal structure as a guide (Perutz, 1970). Lindstrom et al. (1972) have unambiguously assigned the furthest upfield peaks at −1.7 ppm in R-state carbon monoxide Hb to the γ_1-methyl protons of β67-E11-valine and α63-E11-valine, and the next furthest upfield peak at −0.94 ppm to the γ_2-methyl protons of β67-E11-valine. We expected to see at least these three methyl proton peaks in the ZnPChl*a*–heme hybrids; in fact, their spectra each show six peaks, three in the β-chains and three in the α-chains (Figure 4). The γ_1-methyl group of the β67-E11-valine lies on the distal side, 3.0 Å away from the porphyrin plane in the deoxyhemoglobin crystal structure (Perutz, 1970; see Figure 5). This is 1 Å closer to the heme plane than its position in oxyhemoglobin (Perutz, 1970). The γ_1-methyl group of the corresponding α63-E11-valine does not move significantly upon oxygenation and lies 3.8 Å away from the heme plane in the deoxy form. This α-methyl group is also laterally further out from the iron than the β-methyl group. Thus, we expect the furthest upfield peak in the β-chains of T-state $\alpha_2^{Chl}\beta_2^{Chl}$ to be further upfield than the corresponding peak in the α-chains, if they do in fact correspond to the E11 valines. This is exactly what is observed (Figure 4).

We can also compare these peak positions in the ZnPChl*a*-substituted pockets to that of oxyhemoglobin [−2.4 ppm (Ho & Russu, 1981)], if we take into consideration differences in the ring currents. The furthest upfield α^{Chl} peak at −2.21 ppm is 0.2 ppm downfield of the oxyhemoglobin valine peak. This should be compared to ZnPChl*a*–Mb, where the E11-Val peak comes at −2.59 ppm (Wright & Boxer, 1981), which is 0.2 ppm downfield from the peak position in oxyMb (Shulman et al., 1970). Because the γ_1-methyl protons of the

Mb E11-valine (Kendrew & Watson, 1971) samples nearly the same region of ring current fields as the corresponding α-chain valine methyl protons in deoxyhemoglobin, there appears to be a consistent and small effect upon replacing oxyheme by ZnPChl*a*. On the other hand, the large motion of the β67-E11-valine toward the iron upon deoxygenating the β-chain apparently dominates the small ring-substitution effect, and the β^{Chl} peak is in fact observed at −3.03 ppm. This is 0.6 ppm upfield from the valine peak of oxyhemoglobin. Thus, there is an entirely consistent pattern for the relative *and* absolute positions of the −3.03 ppm and the −2.21 ppm peaks in the $\alpha_2^{Chl}\beta_2^{Chl}$, if we assign the former to the γ_1-methyl protons of β67-E11-valine and the latter to the γ_1-methyl protons of α63-E11-valine. Finally, it should be noted that there is a precedent for observing an upfield shift for the β, but not α, diamagnetic ring current shifted E11-valine peak in studies on the effect of anions on the tertiary structure of carbon monoxide hemoglobin (Lindstrom & Ho, 1973).

Two methyl resonances in the upfield NMR region for each chain remain to be assigned. From the crystal-structure coordinates in the deoxyheme crevice (Figure 5), we find that the γ_2-methyl group of the E11-valines and the δ_1-methyl group of the proximal FG3-leucines in both the α- and β-chains are expected to be strongly upfield shifted. These methyl groups are about the same distance away from the heme plane as the γ_1-methyl group of α63-E11-valine and are slightly further out from the iron, and these are the *only* protein methyl groups within that range. Thus, we can tentatively propose that the −1.29 and −1.86 ppm peaks of the β-chain represent the γ_2-methyl protons of the β-E11-valine and the δ_1-methyl protons of β-FG3-leucine, though it is not clear which is which. Likewise, we propose that the −1.86 ppm peak of the α-chain, representing two methyl groups, arises from the two analogous protein methyls in the α-chain.

LaMar and co-workers have suggested that a heterogeneity in reconstituted hemoproteins may occur because the porphyrin can be inserted with a 180° rotation around its α–γ axis, relative to the native position (LaMar et al., 1978). If we are correct in assigning one peak in each chain to the δ_1-methyl of FG3-leucine, then such a rotation is improbable in the chlorophyllide–hemoglobins. This is because a 180° rotation about the α–γ axis of ZnPChl*a* would switch the saturated ring D for the pyrrolic ring C (see Figure 1), which would greatly reduce the ring current shift of the leucine probe. The integrals of the observed peaks, however, are in clean integer ratios with the area of the furthest upfield methyl peak in both the $\alpha_2^{h}(\text{deoxy})\beta_2^{Chl}$ and $\alpha_2^{Chl}\beta_2^{h}(\text{deoxy})$ spectra. Taken as a whole, the existence and details of the upfield region of the ^{1}H NMR spectra of $\alpha_2^{Chl}\beta_2^{Chl}$, $\alpha_2^{Chl}\beta_2^{h}(\text{deoxy})$, and $\alpha_2^{h}(\text{deoxy})\beta_2^{Chl}$ strongly support the claim that ZnPChl*a* has been successfully and specifically inserted into the heme pockets.

Analysis of Fluorescence Anisotropy. Given a solution of randomly oriented ground-state chromophores, the maximum emission anisotropy for a nonrotating fluorophore is $r_{max} = {}^2/_5$ (Jablonski, 1961). If energy transfer to a second, degenerate fluorophore in the chromophore system occurs within the singlet lifetime, this will degrade the anisotropy of the excited state distribution *to the degree* that the dot product of the two normalized transition dipole moments ($\hat{M}_1$ and $\hat{M}_2$) is less than unity. The anisotropy of the emission from a transition dipole, $\hat{M}_2$, *not* initially excited by the incoming light beam is given by

$$r_{D\to A} = (1/5)(3\cos^2\phi - 1) \qquad (1)$$

where $\cos\phi = \hat{M}_1\cdot\hat{M}_2$, and $\hat{M}_1$ is the normalized transition dipole moment that is initially excited (Dale & Eisinger, 1975; Tanaka & Mataga, 1979). The total sample emission exhibits an anisotropy that is simply the average of the monomer anisotropy r_0 ($\sim r_{max}$) and the dimer transfer anisotropy, $r_{D\to A}$, appropriately weighted for their relative steady-state populations.

Table II: Transition Dipole Orientation Calculated from Polarization Data

protein	ϕ[a]	θ, κ^2[b]
$\alpha_2^{Chl}\beta_2^{h}$(deoxy)	33°	102°, 0.39; 141°, 2.20
α_2^{h}(deoxy)β_2^{Chl}	33°	99°, 0.41; 136°, 1.62
$\alpha_2^{Chl}\beta_2^{Chl}$		20°, 40°, 95°, or 150°

[a] cos ϕ is the dot product between the dopoles in the two chains. [b] θ values are the orientations of the transition dipole within the chlorin macrocycle (θ = 0° for the x axis) that fit the polarization data, and associated with the θ are values of κ^2 predicted by eq 2 for that dipole orientation.

Intramolecular nonradiative energy transfer is in fact observed to occur between the ZnPChl*a* chromophores in the three proteins $\alpha_2^{Chl}\beta_2^{Chl}$, $\alpha_2^{Chl}\beta_2^{h}$(deoxy), and α_2^{h}(deoxy)β_2^{Chl}. These multichlorophyll systems exhibit fluorescence anisotropies substantially lower than that of the monomer anisotropy, under conditions where molecular rotation and intermolecular radiative and nonradiative energy transfer have been carefully excluded.

The Förster energy-transfer first-order rate constant, k_t, is given in a convenient form by

$$k_t = (3/2)\kappa^2(R_0/R)^6 k_f \qquad (2)$$

where R is the interchromophore distance (center to center), R_0 is the "Förster critical transfer distance" and is a characteristic of the chromophore pair, k_f is the observed fluorescence lifetime due to all other decay processes, and κ is the orientational factor of the dipole–dipole interaction energy (Förster, 1965). κ^2 is given by

$$\kappa^2 = [\hat{M}_1\cdot\hat{M}_2 - 3(\hat{M}_1\cdot\hat{R})(\hat{M}_2\cdot\hat{R})]^2 \qquad (3)$$

where $\hat{R}$ is the unit vector of the interchromophore vector. The β–β center-to-center distance in deoxyHb is 40.2 Å, the α–α distance is 34.8 Å (Perutz, 1970)[3], and the ZnPChl*a*–ZnPChl*a* R_0 is expected to be about 53 Å (Knox, 1975).[4] Therefore, if we assume that κ^2 does not happen to be less than $\sim{}^1/_3$, k_t is expected to be much faster than k_f [$k_f = (2.5 \pm 0.2) \times 10^8$ s^{-1} for ZnPChl*a*–Mb (Wright & Boxer, 1981)]. This means that the excitation will equilibrate rapidly between the two ZnPChl*a* chromophores of the hybrids during the fluorescence lifetime. To a first approximation, then, half the emitted fluorescence will exhibit the monomer anisotropy, r_0, and half the dimer transfer anisotropy, $r_{D\to A}$.[5] The exact relation in the case of two identical chromophores is

$$r = \frac{k_t r_{D\to A} + (k_f + k_t)r_0}{k_f + 2k_t} \qquad (4)$$

[4] Knox's estimate of the R_0 for magnesium-containing chlorophyll is 58 Å (Knox, 1975); this figure has been adjusted downward for the case of a zinc-containing chlorophyllide, which exhibits a shorter fluorescence lifetime (see k_f in text). This approximate correction assumes that only the nonradiative decay rates have been affected upon replacing magnesium by zinc; this assumption needs to be tested by direct quantum-yield measurements on the ZnPChl*a* proteins. Nevertheless, an approximate value of R_0 suffices for the purposes of the argument.

[5] The approximation that $k_t \gg k_f$ and thus $r = (1/2)(r_0 + r_{D\to A})$ was refined by an iterative method. The values of θ have been passed through a one-step iteration in which κ^2 was calculated, R_0 = 53 Å was assumed, and eq 4 was used to recalculate $r_{D\to A}$ and thus θ. This results in a minor correction of 1° in θ.

where use has been made of the steady-state populations derived by Förster (1948). Equation 4 reduces properly to $r = (1/2)(r_0 + r_{D\rightarrow A})$ in the case of $k_t \gg k_f$.

In combination with eq 1, the geometrical factor, $\phi = \cos^{-1} \hat{M}_1 \cdot \hat{M}_2$, can be extracted simply and is presented in Table II. The absolute accuracy of the anisotropy results can be estimated from the observed glycogen anisotropy of 0.98 by a simple linear relation. For example, when r is observed to be 0.289, it may in fact be 0.289/0.98 = 0.295, which is a minor correction. The uncertainty in the measurement of the anisotropy is listed in Table I and includes a very small contribution from the uncertainty of the emission bias. We believe that the deviation of the *monomeric* ZnPChl*a*–Mb anisotropy, as well as that of oxazine 725, from the ideal value of 0.4 is a *molecular property* (see Appendix).

The essentially identical anisotropies observed for the two hybrids, together with the pseudo-2-fold axis relating the α-chains to the β-chains in the native Hb crystal structure, suggest that ZnPChl*a* is substituting for the heme in the *same manner* into the α- and β-chains, preserving the symmetry.

The dot product of $\hat{M}_1$ and $\hat{M}_2$ can be interpreted in terms of the orientation, θ, of the ZnPChl*a* Q_y transition dipole within the molecular plane by cautiously invoking the deoxyhemoglobin crystal structure. The strength of this assumption lies in the following two facts: (i) the deoxy hybrids are observed to exhibit tertiary and quaternary structural characteristics of T-state deoxyHb; (ii) these characteristics (distinct heme Soret, dissociation equilibrium, PMB kinetics) are unique to T-state deoxyHb among all other states of tetrameric hemoglobins as well as among globins, semihemoglobins, or isolated chains (Antonini & Brunori, 1971). The existence of eight specific salt bridges unique to deoxyHb, which Perutz has identified as a major contributor to the stabilization of the T-state conformation (Perutz, 1970), suggests that the energy minimum with respect to quarternary conformational changes may be a rather narrow one in the fully unligated T state. The weakness of the assumption is that, while the protein may fold around the ZnPChl*a* macrocycle as it does around deoxyheme, a slight in-plane rotation of the ZnPChl*a* macrocycle with respect to the heme porphyrin position cannot be ruled out. As we have argued before (Wright & Boxer, 1981), the ZnPChl*a* ring differs least from the heme ring on the side that is imbedded deeply in the hydrophobic interior of the heme cleft (rings A and B); the major differences occur on the side that is close to the protein–solvent boundary (rings C, D, and E). Thus, the calculated θ could be systematically off by 5–10°, but we can rigorously distinguish X-axis polarization ($\theta = 0°$) from $\theta = 45°$ or from y-axis polarization ($\theta = 90°$). Any residual ambiguity should be eliminated when the X-ray structure of ZnPChl*a*–Mb, presently in progress (Boxer et al., 1982), is completed.

The two macrocycles in the α-chains (or the two in the β-chains) are related by a C_2 symmetry operation, which simplifies the interpretation, but the planes of the macrocycles are not parallel. The dependence of the orientational factors ϕ and κ^2 on the molecular parameter θ was calculated from the x, y, and z coordinates of a vector of orientation θ in the α_1-, α_2-, β_1-, and β_2-chains. Calculated curves for the range of θ that predicts anisotropies comparable to those we have measured (Table I) are shown in Figure 6, for the two hybrids and $\alpha_2^{Chl}\beta_2^{Chl}$. The anisotropy of a rapidly equilibrating $\alpha_2^{Chl}\beta_2^{Chl}$ tetramer is calculated as

$$r = (1/4)r_0 + (1/4)r_{\alpha 1\beta 1} + (1/4)r_{\alpha 1\beta 2} + (1/8)r_{\alpha 1\alpha 2} + (1/8)r_{\beta 1\beta 2} \quad (5)$$

where the C_2 symmetry of the tetramer has been invoked and

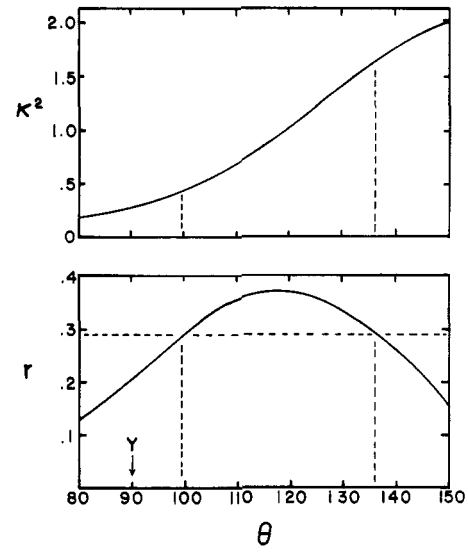

FIGURE 6: Calculated dependences of $\kappa^2(\theta)$ and $r = (1/2)[r_0 + r_{D\rightarrow A}(\theta)]$ on the transition dipole orientation, θ, for $\alpha_2^{h}(\text{deoxy})\beta_2^{Chl}$. Only the range of θ that yields anisotropies comparable to that measured is displayed. The orientation of the chromophores is taken from the deoxyHb crystal structure;[3] see text. The experimental anisotropy for the hybrids is indicated with the horizontal dashed lines ($r = 0.287 \pm 0.003$), and the corresponding values of θ and κ^2 are indicated with vertical dashed lines.

the subscripts refer to the donor–acceptor pair. Ideally, the experimentally measured anisotropies for each molecular system would occur for the identical value of θ (assuming that θ is identical in α- and β-chains). The values for θ that fit the data are shown in Figure 6.[5] It is evident that very close agreement among all three, independently measured proteins is obtained for angles in the range $\theta = 95$–$102°$. A second, less self-consistent solution is found for $\theta = 136$–$150°$. The former range is very close to the y axis of ZnPChl*a*, $\theta = 90°$; the latter is 46–60° away from the y axis. Time-resolved measurements should be able to clearly resolve this ambiguity, as the predicted values of κ^2 differ by a factor of 4 between these two dipole orientations (Table II and Figure 6). This ability to discriminate arises because the orientational dependence of the dimer transfer anisotropy, eq 1, differs from that of dipole–dipole interaction, eq 3. While it is not possible at present to exclude the 136–150° range of angle, it is noteworthy that the value $\theta = 98 \pm 4°$ gives a significantly better fit. Note that the results for $\alpha_2^{Chl}\beta_2^{h}$, $\alpha_2^{h}\beta_2^{Chl}$, and $\alpha_2^{Chl}\beta_2^{Chl}$, are derived from completely independent analyses of independent data on the different proteins.

The theoretical predictions for the Q_y orientation in chlorophyll *a* itself are $\theta = 92°$ (Chang, 1977), $\theta = 89°$ (Weiss, 1972), $\theta = \sim 70°$ (Song et al., 1972), and $\theta = 84.5°$ (Petke et al., 1979). Given the uncertainty in the precise ZnPChl*a*–deoxyheme structural homology, we conclude that our experimental determination is entirely consistent with the theoretical assignment of the main Q_y transition dipole moment to the Y molecular axis ($\theta = 90°$). This theoretical result has hitherto been treated as a first and only approximation. It is evident from the analysis above, and the work of others (Stryer & Haugland, 1965; Zemel & Hoffman, 1981), that the long-range order imposed by a biological macromolecule offers an excellent tool for the resolution of spectroscopic and photophysical problems.

Appendix

The emission anisotropy of randomly oriented, rigid, nonrotating, monomeric fluorophores, r_0, is rarely equal to the

limiting value of the emission anisotropy, 0.4, whether or not the fluorophore is bound to a macromolecule (Dale & Eisinger, 1975; Steinberg, 1975). The reasons for this fall in two classes: the first includes all errors associated with the measurement process; the second endeavors to explain the shortfall as a true molecular property, stripped of experimental artifact. If the monomer anisotropies of oxazine 725 and ZnPChl*a*–Mb (Table I) fall short of 0.4 for molecular reasons, then eq 1 must be modified accordingly. As it stands, the $r_{D\rightarrow A}$ derived from eq 1 becomes exactly 0.4 as $\phi \rightarrow 0$, which is the ideal, but improper, limit. In order to amend the equation to a proper ϕ dependence, it is necessary to propose a molecular model for the deviation of r_0 from 0.4. For example, if we assume that the absorption and emission dipoles are in fact not parallel to each other, the monomer r_0 and eq 1 may be used to calculate the angle between them: 12°. This would be significant in that the meaning of a single orientational parameter, θ, becomes less well defined.

The absolute emission anisotropies observed for the ZnPChl*a* proteins may be corrected for the very small defect revealed by the glycogen scatter anisotropy, 0.983 + 0.003. The actual molecular anisotropy is related to that observed by $r_{mol} > r_{obsd} > 0.98\ (r_{mol})$, which is a very narrow range. We assume the worst case by setting $r_{mol} = r_{obsd}/0.98$. This error includes errors due to any misalignment of polarizers and observation direction or due to any convergence of the excitation beam and divergence of the collected emission. Thus, corrected for maximum experimental artifact, the observed anisotropy of ZnPChl*a* is $r_0 = 0.374 \pm 0.003$ and that for oxazine 725 is almost ideal at $r_0 = 0.393 \pm 0.004$. Though both of these measurements were taken in the experimentally observed limit of infinite viscosity, neither of these systems was a frozen glass in which strains and accompanying depolarization may occur (Steinberg, 1975). Unlike many fluorophores more loosely bound to proteins, the ZnPChl*a* is inserted in a specific crevice "designed" for the very closely related heme macrocycle; thus its emission anisotropy is not expected to be diminished by residual rotational freedom.

It seems quite plausible that the observed small depolarization in ZnPChl*a*–Mb may result from weak vibronic lines within the main Q_y 0–0 band, which derive their intensity through vibronic borrowing (Albrecht, 1961; Herzberg & Teller, 1933). As argued before (Boxer et al., 1982), small vibronic components of differing polarization could underlie the unresolved Q_y 0–0 envelope, particularly toward the short-wavelength side of the absorption band and toward the long-wavelength side of the 0–0 hump in the emission spectrum. Additional depolarization was indeed observed (Table I) when the exciting wavelength was shifted 9 nm to the blue or when the emission monochromator was tuned 9 nm to the red, in both cases staying well within the 0–0 vibronic envelope. On the other hand, narrowing the monochromator slit widths at the absorption peaks had no effect on the measured anisotropy. This suggests that the $r_0 = 0.374$ value observed at the peak is a consequence of the overlapping band shapes of the constituent vibronic lines rather than insufficient resolution in the measurement. We note that oxazine 725, which possesses a near ideal emission anisotropy, has no major higher energy absorption bands until beyond 300 nm and would thus be expected to be much less susceptible to mixed polarization though vibronic coupling.

This interpretation of the limiting anisotropy of ZnPChl*a*–Mb has the following implication. The *principal* components of the absorption and emission Q_y transition dipoles are in fact parallel, but each transition is contaminated with a small amount of a transition dipole component of a differing direction. If this second dipole is taken to be perpendicular to the principal direction, then the relative magnitude of its dipole strength need only be ~2% of that of the principal dipole in order to explain the observed r_0. Equation 1 may be modified to include a major and minor dipole on both the donor and acceptor, and recalculation of θ then results in an insignificant change of 1° in the case of our anisotropy data. On the other hand, the assumption that the absorption and emission dipoles on each chromophore are single nonparallel vectors separated by an angle λ leads to the following expression (Tao, 1969):

$$r_{D\rightarrow A} = (P_2 \cos \lambda)(3 \cos^2 \phi - 1)/5 \qquad (A1)$$

λ in our case would have to be 12° and $P_2(\cos \lambda) = 0.935$. For the reasons stated above, we do not make this assumption, and the emission and absorption transition dipoles in this rigid macrocycle are taken to be well-defined by a single principal orientation, θ.

Added in Proof

Time-resolved fluorescence decay measurements have revealed that the hybrid ZnPChl*a*–deoxyheme hemoglobins exhibit a markedly shorter ZnPChl*a* fluorescence lifetime (1.4 ns) than either the ZnPChl*a*–Mb (3.9 ns) or $\alpha_2^{Chl}\beta_2^{Chl}$ (3.7 ns) proteins. This can be accounted for by energy transfer from ZnPChl*a* to weak low-lying bands of the deoxyheme by a Förster dipole–dipole mechanism. This will also result in small refinements of the orientation θ, which will be presented in an upcoming paper on time-resolved measurements.

References

Ackers, G. K. (1967) *J. Biol. Chem. 242*, 3026–3034.

Adar, F., Gouterman, M., & Aronowitz, S. (1976) *J. Phys. Chem. 80*, 2184–2191.

Albrecht, A. C. (1961) *J. Mol. Spectrosc. 6*, 84–108.

Alpert, B. (1972) *C. R. Hebd. Seances Acad. Sci., Ser. D 275*, 1179–1182.

Amrein, W., & Shaffner, K. (1975) *Helv. Chim. Acta 58*, 397–415.

Antonini, E., & Brunori, M. (1969) *J. Biol. Chem. 244*, 3909–3912.

Antonini, E., & Brunori, M. (1971) *Hemoglobin and Myoglobin and Their Reaction with Ligands*, North-Holland, Amsterdam.

Bär, F., Lang, H., Schnabel, E., & Kuhn, H. (1961) *Z. Electrochem. 65*, 346–354.

Bolton, W., & Perutz, M. F. (1970) *Nature (London) 228*, 551.

Boxer, S. G., & Roelofs, M. (1979) *Proc. Natl. Acad. Sci. U.S.A. 76*, 5635–5640.

Boxer, S. G., & Wright, K. A. (1979) *J. Am. Chem. Soc. 101*, 6791–6794.

Boxer, S. G., Kuki, A., Wright, K. A., Katz, B. A., & Xuong, N. H. (1982) *Proc. Natl. Acad. Sci. U.S.A. 79*, 1121–1125.

Boyer, P. D. (1954) *J. Am. Chem. Soc. 76*, 4331–4337.

Bücher, H., Drexhage, K. H., Fleck, M., Kuhn, H., Möbius, D., Schäfer, F. P., Sondermann, J., Sperling, W., Tillman, P., & Wiegand, J. (1967) *Mol. Cryst. 2*, 199–230.

Buchler, J. W. (1975) in *Porphyrins and Metalloporphyrins* (Smith, K. M., Ed.) pp 157–231, Elsevier Scientific, New York.

Bucks, R. R., & Boxer, S. G. (1982) *J. Am. Chem. Soc. 104*, 340–343.

Bunting, J. R., & Filipescu, N. (1970) *J. Chem. Soc. B*, 1750–1755.

Chang, J. C. (1977) *J. Chem. Phys. 67*, 3901–3909.

Chu, A. H., & Ackers, G. K. (1981) *J. Biol. Chem. 256*, 1199–1205.
Dale, R., & Eisinger, J. (1975) in *Biochemical Fluorescence: Concepts* (Chen, R. F., & Edelhock, H., Eds.) Vol. I, p 91, Marcel Dekker, New York.
Davis, R. C., & Pearlstein, R. M. (1979) *Nature (London) 280*, 413–415.
Eaton, W. A., & Hofrichter, J. (1981) *Methods Enzymol. 76*, 175–261.
Filipescu, N., DeMember, J. R., & Minn, F. L. (1969) *J. Am. Chem. Soc. 91*, 4169–4173.
Förster, Th. (1948) *Ann. Phys. (Leipzig) 2*, 55–75.
Förster, T. H. (1965) in *Modern Quantum Chemistry* (Sinanoglu, O., Ed.) Vol. III, pp 93–137, Academic Press, New York.
Frank, H. A., Friesner, R., Nairn, J. A., Dismukes, C., & Sauer, K. (1979) *Biochim. Biophys. Acta 546*, 347.
Friedman, F. K., Alston, K., & Schechter, A. N. (1981) *Anal. Biochem. 117*, 103–107.
Furhop, J. H., & Smith, K. M. (1975) in *Porphyrins and Metalloproteins* (Smith, K. M., Ed.) p 798, Elsevier, Amsterdam.
Geraci, G., Parkhurst, L. J., & Gibson, Q. H. (1969) *J. Biol. Chem. 244*, 4664–4667.
Gouterman, M., & Stryer, L. (1962) *J. Chem. Phys. 37*, 2260–2266.
Guêron, M. (1975) *J. Magn. Reson. 19*, 58–66.
Guidotti, G. (1967) *J. Biol. Chem. 242*, 3673.
Herzberg, G., & Teller, E. (1933) *Z. Phys. B 21*, 410–446.
Hinson, J. A., & McMeekin, T. L. (1969) *Biochem. Biophys. Res. Commun. 35*, 94–101.
Ho, C., & Russu, I. M. (1981) *Methods Enzymol. 76*, 275–312.
Hoffman, B. M. (1979) in *The Porphyrins* (Dolphin, D., Ed.) Vol. 7, pp 403–444, Academic Press, New York.
Hwang, P. H., & Greer, J. (1980) *J. Biol. Chem. 255*, 3008–3041.
Ikeda-Saito, M., Inubushi, T., McDonald, G. G., & Yonetani, T. (1978) *J. Biol. Chem. 253*, 7134–7137.
Jablonski, A. (1961) *Z. Naturforsch., A 16*, 1–4.
Johnson, M. E., Fung, L. W.-M., & Ho, C. (1977) *J. Am. Chem. Soc. 99*, 1245–1250.
Jortner, J. (1980) *Biochim. Biophys. Acta 594*, 193–230.
Kasha, M., Rawls, H. R., & El-Bayoumi, M. A. (1965) *Pure Appl. Chem. 11*, 371–392.
Keller, R. A. (1968) *J. Am. Chem. Soc. 90*, 1940–1944.
Kendrew, J. C., & Watson, H. C. (1971) in *Hemoglobin and Myoglobin in Their Reactions with Ligands* (Antonini, E., & Brunori, M., Eds.) p 85, North-Holland, Amsterdam.
Kirshner, A. G., & Tanford, C. (1964) *Biochemistry 3*, 291.
Knox, R. S. (1975) in *Bioenergetics of Photosynthesis* (Govindjee, Ed.) pp 183–221, Academic Press, New York.
Koka, P., & Song, P. S. (1977) *Biochim. Biophys. Acta 495*, 220–231.
LaMar, G. N., Budd, D. L., Viscio, D. B., Smith, K. M., & Langry, K. C. (1978) *Proc. Natl. Acad. Sci. U.S.A. 75*, 5755–5759.
Lamola, A. A. (1969) *J. Am. Chem. Soc. 91*, 4786–4790.
Leonard, J. L., Yonetani, T., & Callis, J. B. (1974) *Biochemistry 13*, 1460–1464.
Lindstrom, T. R., & Ho, C. (1973) *Biochemistry 12*, 134–139.
Lindstrom, T. R., Noren, I. B. E., Charache, S., Lehman, H., & Ho, C. (1972) *Biochemistry 11*, 1677–1681.
Matthews, B. W., & Fenna, R. E. (1979) in *The Porphyrins* (Dolphin, D., Ed.) Vol. 7, Academic Press, New York.
Matthews, B. W., & Fenna, R. E. (1980) *Acc. Chem. Res. 13*, 309–317.
Muirhead, H., & Greer, J. (1970) *Nature (London) 228*, 516–519.
Netzel, T. L., Bergkamp, M. A., & Chang, C. K. (1982) *J. Am. Chem. Soc. 104*, 1952–1957.
Ogawa, S., & Shulman, R. G. (1972) *J. Mol. Biol. 70*, 315–336.
Perutz, M. F. (1970) *Nature (London) 228*, 726–734.
Petke, J. D., Maggiora, G. M., Shipman, L. L., & Christofferson, R. E. (1979) *Photochem. Photobiol. 30*, 203–223.
Rafferty, C. N., & Clayton, R. K. (1979) *Biochim. Biophys. Acta 546*, 189–206.
Seely, G. R. (1970) *J. Phys. Chem. 74*, 219–227.
Sevchenko, A. N., Solov'ev, K. N., Mashenkov, V. A., Shkirman, S. F., & Losev, A. P. (1968) *Sov. Phys.—Dokl. (Engl. Transl.) 12*, 787–789.
Shulman, R. G., Wüthrich, K., Yamane, T., Patel, D. J., & Blumberg, W. E. (1970) *J. Mol. Biol. 53*, 143–157.
Song, P.-S., Moore, T. A., & Sun, M. (1972) in *Chemistry of Plant Pigments* (Chichester, C. O., Ed.) pp 33–74, Academic Press, New York.
Steinberg, I. Z. (1975) in *Biochemical Fluorescence: Concepts* (Chen, R. F., & Edelhock, H., Eds.) Vol. I, Marcel Dekker, New York.
Strain, H. H., & Svec, W. A. (1966) in *The Chlorophylls* (Vernon, L. P., & Seely, G. R., Eds.) Chapter 2, Academic Press, New York.
Stryer, L., & Haugland, R. P. (1967) *Proc. Natl. Acad. Sci. U.S.A. 58*, 719–726.
Tanaka, F., & Mataga, N. (1979) *Photochem. Photobiol. 29*, 1091–1097.
Tao, W. (1969) *Biopolymers 8*, 609–632.
Teale, F. W. J. (1959) *Biochim. Biophys. Acta 35*, 543.
Thurnauer, M. C., & Norris, J. R. (1976) *Biochem. Biophys. Res. Commun. 73*, 501.
Thurnauer, M. C., & Norris, J. R. (1977) *Chem. Phys. Lett. 47*, 100.
Tyer, N. W., Jr., & Becker, R. S. (1970) *J. Am. Chem. Soc. 92*, 1295–1302.
Waks, M., Yip, Y. K., & Beychok, S. (1973) *J. Biol. Chem. 248*, 6462–6470.
Waterman, M. R., & Yonetani, T. (1970) *J. Biol. Chem. 245*, 5847–5852.
Weiss, C. (1972) *J. Mol. Spectrosc. 44*, 37–80.
Winterhalter, K. H. (1966) *Nature (London) 211*, 932–934.
Winterhalter, K. H., & Deranleau, D. A. (1967) *Biochemistry 6*, 3136–3143.
Wright, K. A., & Boxer, S. G. (1981) *Biochemistry 20*, 7546–7556.
Yip, Y. K., Waks, M., & Beychok, S. (1977) *Proc. Natl. Acad. Sci. U.S.A. 74*, 64–68.
Yonetani, T. (1967) *J. Biol. Chem. 242*, 5008–5013.
Zemel, H., & Hoffman, B. M. (1981) *J. Am. Chem. Soc. 103*, 1192–1201.
Zimmerman, H. E., Goldman, T. D., Hirzel, T. K., & Schmidt, S. P. (1980) *J. Org. Chem. 45*, 3933–3951.